Origin of clear ferromagnetism for *p*-type GaN implanted with Fe^+ (5 and 10 at. %)

Yoon Shon,[a),b)] Sejoon Lee,[c)] H. C. Jeon, Y. S. Park, D. Y. Kim, and T. W. Kang
Quantum-Functional Semiconductor Research Center, Dongguk University, Seoul 100-715, Korea

Jin Soak Kim and Eun Kyu Kim[a),d)]
Department of Physics, Hanyang University, Seoul 133-791, Korea

D. J. Fu and X. J. Fan
Department of Physics, Wuhan University, Wuhan 430072, People's Republic of China

Y. J. Park
Nano Device Research Center, Korea Institute of Science and Technology, Seoul 130-650, Korea

J. M. Baik and J. L. Lee
Department of Materials Science and Engineering, Pohang University of Science and Technology, Kyungbuk 790-784, Korea

(Received 10 June 2006; accepted 30 June 2006; published online 22 August 2006)

The systematic enhancement of ferromagnetic hysteresis loops for GaN implanted with high doses of Fe ($5 \rightarrow 10$ at. %) takes place with an increase in the annealing temperature from 700 to 850 °C. The trends of magnetic properties coincide with the results of the increased full width at half maximum of triple axis diffraction for GaN (0002), including the appearance of GaFeN, the enhanced Fe-related photoluminescence transitions, and the systematic increase in sizes of symmetric spin ferromagnetic domains GaFeN in atomic force microscopy and magnetic force microscopy. © *2006 American Institute of Physics*. [DOI: 10.1063/1.2338000]

According to a recent theory based on the Zener model with a Mn concentration of 5% per cation in 2^+ charge state and 3.5×10^{20} holes/cm^3,[1] Mn-doped GaN and ZnO have high Curie temperature (T_C) above 300 K and many experimental studies have been actively carried out.[2–10] Meanwhile, according to another double exchange model,[11] the total energy (TE) within the local spin density approximation was calculated for both $(Ga_{1-x}TM_x^{\uparrow})N$ and $(Ga_{1-x}TM_{x/2}^{\uparrow}TM_{x/2}^{\downarrow})N$ as a function of x. TM indicates transition metal. Then ΔE=TE (spin glass state) −TE (ferromagnetic state). For x=5%, 10%, 15%, 20%, and 25%, the ferromagnetic states were also stable in GaNMn, GaNV, and GaNCr, but GaNFe, GaNCo, and GaNNi showed spin glass states. Particularly, GaNFe did not show a ferromagnetic state for all values of x. However, in contrast with the theory, ferromagnetic properties in GaNFe layer have been recently reported.[12–15]

The Mg-doped GaN films were grown on *c*-plane sapphire (Al_2O_3) substrates by MOCVD. The thickness of the GaN:Mg epilayers was 1500 nm. The Hall effect measurement of GaN:Mg epilayers showed *p*-type conductivity with a carrier concentration of 3×10^{17} cm^{-3}. The *p*-type GaN epilayers grown by MOCVD were also uniformly implanted with Fe ions at an energy of 200 keV, and the doses were 1×10^{16} cm^{-2} (5%) and 5×10^{16} cm^{-2} (10%). After the implantation of Fe^+, the rapid thermal annealing of *p*-type GaN epilayers was performed in a flowing nitrogen atmosphere, and the annealing temperatures were varied between 700 and 850 °C for a fixed annealing time of 30 s.

Inset (a) of Fig. 1 shows the XRD patterns for the as-grown, as-implanted GaFeN epilayers and the GaFeN epilayers annealed at 700, 800, and 850 °C for 30 s with Fe concentration of 10%. The as-grown epilayer showed only GaN (0002) peak at 34.2°. After the implantation of Fe with doses of 5% and 10%, GaN (0002) peak at 34.2° which appeared in the as-grown epilayers disappeared as the crystallinity was damaged due to the acceleration energy and high doses of heavy ion. After the annealing at 700, 800, and 850 °C subsequent to Fe implantation of 5% and 10%, no secondary phases were observed[12] and the crystallinity of the epilayers including GaFeN is recovered. However, the full width at half maximum (FWHM) of diffraction peaks was increased in comparison with that of the as-grown epilayer. These increases are attributed to the partly *residual lattice damage from the implantation* of injected Fe, together with the formation of GaFeN. The formation of GaFeN is supported by the following discussion and the AFM and MFM images.

Inset (b) of Fig. 1 shows the double crystal x-ray rocking curve (DCRC) of GaN (0002) plane measured to investigate the change of FWHM due to the injection of Fe. The FWHM of DCRC for the as-grown epilayer was 383.3 arc sec. The FWHM of DCRC for the sample annealed at 700 °C for 30 s with Fe concentration of 10% was 544.2 arc sec and increased in comparison with that of the as-grown epilayer (383.3 arc sec) due to the injection of Fe. The ionic raddi of Ga, N, Mg, and Fe are 1.41, 0.7, 1.6, and 1.27 Å, respectively. Fe (ionic radius: 1.27 Å) must substitute for Ga (ionic radius: 1.41 Å) as the molar refractivity of an ion is proportional to the cube of its radius. Therefore, the FWHM of DCRC increases because heavy Fe was properly incorpo-

[a)]Authors to whom correspondence should be addressed.
[b)]Electronic mails: son-yun@hanmail.net and sonyun@dongguk.edu
[c)]Present address: Institute of Industrial Science, University of Tokyo, Tokyo 153-8505, Japan.
[d)]Electronic mail: ek-kim@hanyang.ac.kr

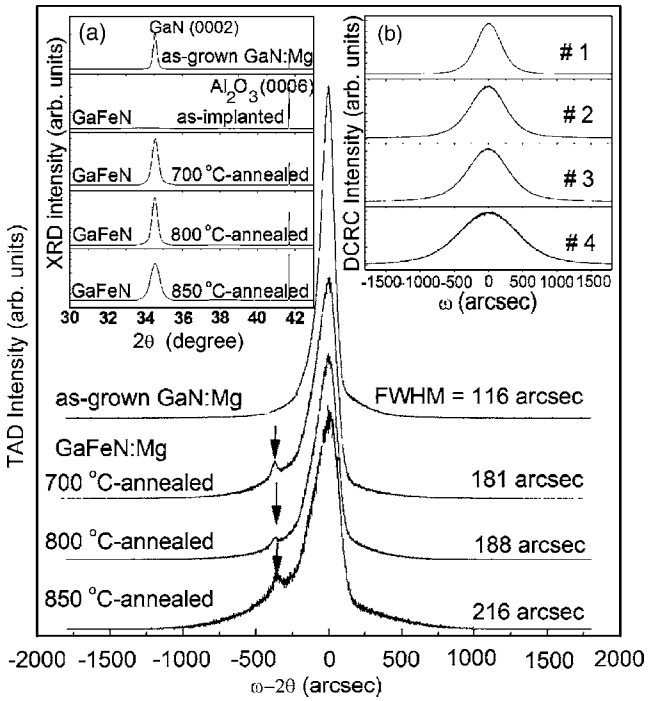

FIG. 1. TAD of GaN (0002) plane measured in order to confirm the existence of GaFeN for epilayers with Fe of 10%. Inset (a) showed XRD patterns for the as-grown GaN and as-implanted and GaFeN epilayers with Fe concentration of 10%. Inset (b) showed DCRC of GaN (0002) measured to investigate the change of FWHM due to the injection of Fe (10%), 1; as-grown GaN:Mg, 2; 700 °C, 3; 800 °C, 4; and 850 °C.

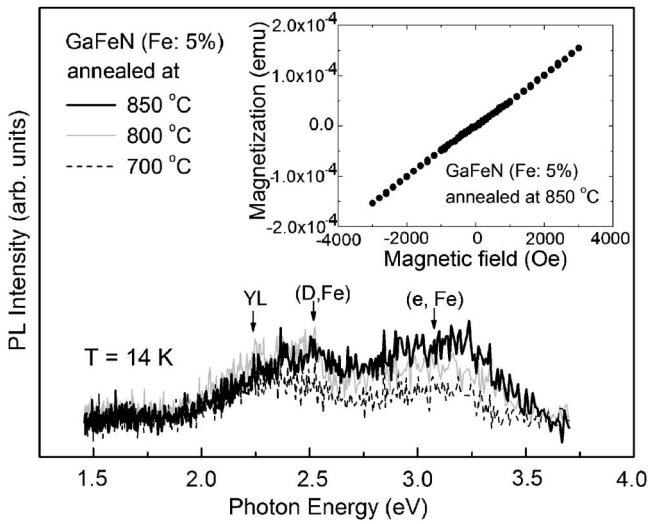

FIG. 2. PL spectra measured at 14 K for the GaFeN epilayers with the Fe concentration of 5%. The inset shows the paramagnetic behavior of the GaFeN epilayer annealed at 850 °C with Fe concentration of 5%.

rated into GaN so as to form GaFeN. With an increase in the annealing temperature from 700 to 800 °C, the FWHM gradually increased from 544.2 to 620.2 arc sec. With an increase in the annealing temperature to 850 °C, the FWHM increased considerably to 872.5 arc sec in comparison with the samples annealed at 700 and 800 °C. These trends coincide with those of PL, AFM and MFM, and SQUID discussed later.

Figure 1 shows the triple axis diffraction (TAD) of GaN (0002) measured in order to confirm the existence of GaFeN based on the above results of DCRC. The as-grown epilayer showed only the peak related to GaN. However, all samples annealed at 700, 800, and 850 °C with Fe concentration of 10% revealed the shoulder peaks of GaFeN, together with GaN (0002) peak. The increases of FWHM for GaN (0002) in TAD also proportionally agreed with those in DCRC with increasing annealing temperature. However, the epilayers with Fe concentration of 5% showed the weak and unreliable changes for the FWHM of DCRC, and TAD did not reveal the shoulder peaks of GaFeN at all. These results agree with the results that the PL transitions of Fig. 2 appear very weakly and the magnetizations of SQUID show paramagnetic behavior, and also the clear, uniform ferromagnetic domains of AFM and MFM images are not formed.

Figure 2 and inset shows PL spectra measured at 14 K and magnetization curve measured at 10 K, respectively. All samples annealed at 700, 800, and 850 °C with Fe concentration of 5% showed three kinds of transitions around 2.25, 2.5, and 3.1 eV. The transition at 2.25 eV is typical YL commonly appeared in GaN. The transitions at 2.5 and 3.1 eV correspond to (*D*, Fe) and (,*e* Fe), respectively. The (*D*, Fe) means a donor–Fe acceptor pair transition and (*e*, Fe) means a conduction band–Fe acceptor transition. The broad peak (*e*, Fe) at 3.1 eV appears to arise from the recombination of free electron with hole bound at a state which is at the energy of 0.4 eV above the valence band edge in terms of an energy level scheme for Fe, namely, peaks at 3.1 eV (E_v+0.4 eV) based on band gap energy of 3.5 eV at 0 K. Therefore, Fe acceptor exists at about E=400 meV in ferromagnetic GaFeN. Although three PL peaks appeared in all samples, the PL intensities were very weak and noisy; namely, Fe-related transition was not properly activated. In proportion to PL transitions, the magnetic properties of all epilayers showed also paramagnetic behaviors in spite of the removal of diamagnetic background (see inset of Fig. 2). Meanwhile, the epilayers implanted with Fe concentration of 10% gradually showed clear, intensive transitions related to Fe with an increase in the annealing temperature from 700 to 850 °C (Ref. 15) consistent with the trends of XRD, AFM and MFM images, and SQUID.

Figure 3 shows the results of room-temperature AFM (left column) and the corresponding MFM (right column) images so as to confirm the existence of ferromagnetic domain. The AFM images of Figs. 3(a)–3(c) showed the topography of the epilayer surface in all the epilayers with Fe concentration of 10% and the formation of the GaFeN domains. And also, the corresponding MFM images revealed the ferromagnetic domains generated and the formation of the ferromagnetic spin domains GaFeN judged by the appearance of dark and bright patterns. The epilayers with Fe concentration of 5% did not produce the clear, uniform ferromagnetic domain images of AFM and MFM images. This result agrees with the results of XRD, PL, and SQUID. The epilayer annealed at 700 °C with Fe concentration of 10% showed the relatively uniform and symmetric ferromagnetic domains of GaFeN, but the ferromagnetic domains are relatively small and unclear. With an increase in the annealing temperature to 800 °C, the ferromagnetic domains of GaFeN layer were improved in comparison with those of epilayer annealed at 700 °C. With an increase in the annealing temperature to 850 °C, the ferromagnetic domains increased in comparison with those of the above two epilayers. Consequently, the symmetric ferromagnetic domains of GaFeN were gradually and systematically improved. The trend of

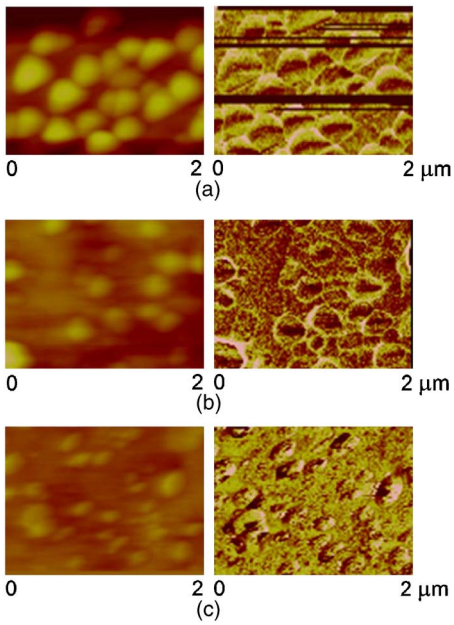

FIG. 3. (Color online) Room-temperature AFM (left column) and MFM (right column) images of GaFeN epilayers annealed at 700 °C (a), 800 °C (b), and 850 °C (c) with Fe concentration of 10% so as to confirm the existence of ferromagnetic domains.

these results coincides with that of the results of XRD and PL discussed above, together with SQUID discussed below.

Based on the results of XRD, PL, and AFM and MFM, the magnetic property has been characterized by SQUID magnetometer measurements. Figure 4 shows the *M-H* curves for GaFeN (10 at. % of Fe). The measurement of hysteresis loop at 10 K was accomplished for the samples annealed between 700 and 850 °C for 30 s and ferromagnetic hysteresis loops were obtained. Ferromagnetic hysteresis loop began to appear in the epilayer annealed at 700 °C but was relatively weak. A coercive field H_c and a remnant field H_r were 143 G and 3.29×10^{-6} emu, and saturation magnetization M_s was 2.17×10^{-5} emu. With an increase in the annealing temperature to 800 and 850 °C, ferromagnetic hysteresis loops continued to increase. The H_c, H_r, and M_s of epilayer annealed at 850 °C apparently increased to 351 G, 1.43×10^{-5} emu, and 7.36×10^{-5} emu. The magnetic properties of ferromagnetic hysteresis loops including H_c, H_r, and M_s increased systematically with an increase in the annealing temperature from 700 to 850 °C. The inset of Fig. 4 shows the hysteresis loop at 300 K for the sample annealed at 850 °C for 30 s so as to confirm magnetization at room temperature. Although a hysteresis loop measured at 300 K was weaker than that at 10 K, a clear hysteresis loop was observed.

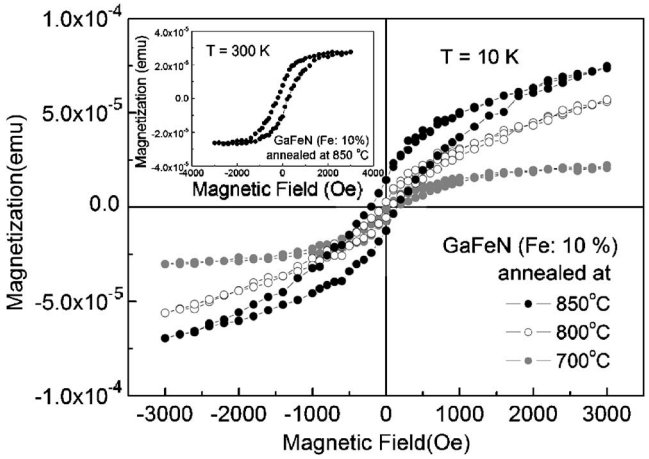

FIG. 4. Ferromagnetic hysteresis loops measured at 10 K with Fe concentration of 10%. The inset shows the ferromagnetic hysteresis loop measured at 300 K for the GaFeN epilayer annealed at 850 °C for 30 s.

In summary, in the case of Fe concentration of 5%, the magnetic properties of all epilayers show paramagnetic behavior. These results agree with those that the TAD of XRD do not produce the shoulders of GaFeN and the Fe-related PL transitions happen very weakly, and also AFM and MFM images do not reveal clear, symmetric ferromagnetic domains. However, the systematic enhancement of ferromagnetic hysteresis loops takes place with an increase in the Fe concentration ($5\rightarrow10$ at. %) and in the annealing temperature from 700 to 850 °C. The trends of magnetic properties coincide with those of results that the shoulders of GaFeN in TAD appear together with the increases of FWHM in DCRC for GaN (0002). The Fe-related PL transitions are enhanced and the sizes of symmetric ferromagnetic domains in AFM and MFM increase systematically with an increase in the annealing temperature from 700 to 850 °C.

This work was supported by the Korea Science and Engineering Foundation (KOSEF) through the Quantum-Functional Semiconductor Research Center (QSRC) at Dongguk University, Research Fund of Dongguk University in 2006, KOSEF National Research Laboratory (NRL) program at Hanyang University, and National Natural Science Foundation of China Contract No. 50175082.

[1] T. Dietl, H. Ohno, F. Matsukura, J. Cibert, and D. Ferrand, Science **287**, 1019 (2000).
[2] M. Zajac, R. Doradzinski, J. Gosk, J. Szczytko, M. Lefeld, M. Kaminska, A. Twardowski, M. Palczewska, E. Granka, and W. Gebicki, Appl. Phys. Lett. **78**, 1276 (2001).
[3] G. T. Thaler, M. E. Overberg, B. P. Gila, R. Franzier, C. R. Albernathy, S. J. Pearton, J. S. Lee, S. M. Lee, Y. D. Park, Z. G. Khim, J. Kim, and F. Ren, Appl. Phys. Lett. **80**, 3964 (2002).
[4] Y. Shon, Y. H. Kwon, Sh. U. Yuldashev, J. H. Lim, C. S. Park, D. J. Fu, H. J. Kim, T. W. Kang, and X. J. Fan, Appl. Phys. Lett. **81**, 1845 (2002).
[5] K. Ando, Appl. Phys. Lett. **82**, 100 (2003).
[6] J. Kim, F. Ren, G. T. Thaler, R. Frazier, C. R. Abernathy, S. J. Pearton, J. M. Zavada, and R. G. Whilson, Appl. Phys. Lett. **82**, 1565 (2003).
[7] M. Marques, L. K. Teles, L. M. R. Scolfaro, J. Furthmüller, F. Bechstedt, and L. G. Ferreira, Appl. Phys. Lett. **86**, 164105 (2005).
[8] J. M. Baik, Y. Shon, T. W. Kang, and J.-L. Lee, Appl. Phys. Lett. **87**, 42105 (2005).
[9] D. P. Norton, S. J. Pearton, A. F. Hebard, N. Theodoropoulou, L. A. Boatner, and R. G. Wilson, Appl. Phys. Lett. **82**, 239 (2003).
[10] S. Lee, Y. Shon, S.-W. Lee, S. J. Hwang, H. S. Lee, T. W. Kang, and D. Y. Kim, Appl. Phys. Lett. **88**, 212513 (2006).
[11] K. Sato and H. Katayama-Yoshida, Jpn. J. Appl. Phys., Part 2 **40**, L485 (2001).
[12] N. Theodoropoulou, A. F. Hebard, S. N. G. Chu, M. E. Overberg, C. R. Albernathy, S. J. Pearton, R. G. Wilson, and J. M. Zavada, Appl. Phys. Lett. **79**, 3452 (2001).
[13] N. Theodoropoulou, M. E. Overberg, S. N. G. Chu, A. F. Hebard, C. R. Abernathy, R. G. Wilson, J. M. Zavada, K. P. Lee, and S. J. Pearton, Phys. Status Solidi B **228**, 337 (2001).
[14] S. J. Pearton, C. R. Albernathy, M. E. Overberg, G. T. Thaler, D. P. Norton, N. Theodoropoulou, A. F. Hebard, Y. D. Park, F. Ren, J. Kim, and L. A. Boatner, J. Appl. Phys. **93**, 1 (2003).
[15] Y. Shon, Y. H. Kwon, Y. S. Park, Sh. U. Yuldashev, S. J. Lee, C. S. Park, K. J. Chung, S. Y. Yoon, H. J. Kim, W. C. Lee, D. J. Fu, T. W. Kang, X. J. Fan, Y. J. Park, and H. T. Oh, J. Appl. Phys. **95**, 761 (2004).